Modulation of Intramolecular Interactions in Superhelical DNA by Curved Sequences: A Monte Carlo Simulation Study

Konstantin V. Klenin,* Maxim D. Frank-Kamenetskii,‡ and Jörg Langowski§
* TRINITI, Troitsk, Moscow Region, 142092, Russia; ‡ Center for Advanced Biotechnology and Department of Biomedical Engineering, Boston University, Boston, Massachusetts 02215 USA; § Deutsches Krebsforschungszentrum, D-69120 Heidelberg, FRG

ABSTRACT A Monte Carlo model for the generation of superhelical DNA structures at thermodynamic equilibrium (Klenin et al., 1991; Vologodskii et al., 1992) was modified to account for the presence of local curvature. Equilibrium ensembles of a 2700-bp DNA chain at linking number difference $\Delta Lk = -15$ were generated, with one or two permanent bends up to 120° inserted at different positions. The computed structures were then analyzed with respect to the number and positions of the end loops of the interwound superhelix, and the intramolecular interaction probability of different segments of the DNA. We find that the superhelix structure is strongly organized by permanent bends. A DNA segment with a 30° bend already has a significantly higher probability of being at the apex of a superhelix than the control, and for a 120° bend the majority of DNAs have one end loop at the position of the bend. The entropy change due to the localization of a 120° permanent bend in the end loop is estimated to be -17 kJ mol^{-1} K^{-1}. When two bends are inserted, the conformation of the superhelix is found to be strongly dependent on their relative positions: the straight interwound form dominates when the two bends are separated by 50% of the total DNA length, whereas the majority of the superhelices are in a branched conformation when the bends are separated by 33%. DNA segments in the vicinity of the permanent bend are strongly oriented with respect to each other.

INTRODUCTION

There is accumulating evidence that structural deformations play a key role in mediating intramolecular interactions in DNA. A recent review (Crothers, 1993) summarizes the effect of protein-mediated DNA bending in the assembly of nucleoprotein complexes; many different proteins involved in such complex formations, such as HU, IHF, HMG-1, or TATA-binding protein, have now been shown to bend DNA. Furthermore, in a number of cases (Bracco et al., 1989; Gartenberg and Crothers, 1991; Goodman and Nash, 1989; Pérez-Martín and Espinosa, 1991) it has been shown that the action of a DNA-bending protein can be mimicked by the insertion of a curved DNA sequence. An intriguing possible biological role of DNA curvature is therefore the steering of intramolecular interactions.

Torsionally stressed DNA under physiological conditions will fold into an interwound superhelix. In such a configuration, one or more end loops exist where the double helix folds back on itself and is much more strongly bent than in other places. There is evidence from electron microscopy (Laundon and Griffith, 1988) and more indirectly from dynamic light scattering (Kremer et al., 1993) that the end loops of a superhelix form preferentially at permanently curved DNA segments. When the position of the end loop is fixed, the relative orientation of DNA segments in its vicinity is also defined. Thus, interactions between DNA segments that are distant on the sequence can be greatly enhanced. Although superhelicity in general is predicted to enhance intramolecular interactions in DNA (Vologodskii et al., 1992), localization of the end loop will have an even greater effect, as we show here.

To understand the mechanism by which DNA-bending proteins can change the structure of larger DNA domains, it becomes important to have quantitative theories of the effect of local structural transitions on the global conformation of superhelical DNA. Considerable progress has been achieved in recent years in computer modeling of DNA molecules under topological constraints (Chirico and Langowski, 1992, 1994; Chirico et al., 1993; Hao and Olson, 1989; Klenin et al., 1988, 1991; Tan and Hanvey, 1989; Schlick and Olson, 1992; Vologodskii et al., 1992; Vologodskii and Frank-Kamenetskii, 1992). A very simple model, which has proved to be remarkably efficient, treats DNA as a homogeneous isotropic elastic rod characterized by three parameters: bending and torsional rigidity constants and the DNA effective diameter. Within the framework of this model one can generate by a Monte Carlo method a statistically correct ensemble of circular DNA chains at thermodynamic equilibrium, allowing for the topological constraints. From there we could obtain reliable theoretical predictions about DNA knotting and supercoiling (Klenin et al., 1988, 1989; Vologodskii et al., 1992; Vologodskii and Frank-Kamenetskii, 1992). These predictions have been extensively used to analyze experimental data on DNA knots and supercoils both qualitatively and quantitatively (Bednar et al., 1994; Vologodskii et al., 1992; Shaw and Wang, 1993; Rybenkov et al., 1993; Langowski et al., 1994). The remarkable agreement between theoretical and experimental data leaves no doubt that the simple model is a very good first approximation to real DNA.

However, the inevitable limitations of the simple model are also evident. First and foremost, it completely ignores permanent curvature of the DNA axis, which is believed to

Received for publication 8 August 1994 and in final form 26 October 1994.
Address reprint requests to Dr. Maxim Frank-Kamenetskii, Center for Advanced Biotechnology, Boston University, 36 Cummington Street, Boston MA 02215. Tel.: 617-353-8498; Fax: 617-353-8501; e-mail: mfk@enga.bu.edu.

0006-3495/95/01/81/08 $2.00

play an important role in DNA functioning, as elaborated above. Therefore, to make the model applicable to a wider range of situations of high biological significance, we have modified the original model to allow for bent sites. Several attempts have been undertaken to introduce permanent bends into various theoretical models of supercoiled DNA (Bauer et al., 1993; Tobias and Olson, 1993; Yang et al., 1993) In the present paper we introduce bends into our Monte Carlo model of DNA supercoiling (Klenin et al., 1991; Vologodskii et al., 1992) and present some results obtained with it. In particular, we can give for the first time a theoretical estimate of the influence of DNA curvature on the intramolecular interaction probability in a superhelix. We show that sequences that are symmetrical with respect to the permanent bend interact more strongly, whereas sequences that are not symmetrical interact less strongly than without the curve.

MATERIALS AND METHODS

Chain structure and energy of the model

The computational procedure used in this study is based on the algorithm by Vologodskii et al. (1992). The DNA model described there requires five independent parameters to define completely the statistical behavior of a supercoiled DNA, 1) the Kuhn statistical length, b; 2) the torsional rigidity, C; 3) the DNA contour length, L; 4) the effective diameter of the double helix, d; 5) the linking number difference, ΔLk. A closed circular DNA molecule is represented by a closed chain consisting of $N = k \cdot L/b$ straight segments of equal length, where k, the number of segments per Kuhn length, is a parameter that is chosen large enough so that the results do not depend on its choice.

To construct a proper statistical set of DNA conformations, the classical Metropolis Monte Carlo procedure is used (Metropolis et al., 1953). The energy of any given chain configuration is the sum of two terms:

$$E = E_b + E_t. \tag{1}$$

The first term is the bending energy:

$$E_b = k_B T \cdot \alpha \cdot \sum_{j=1}^{N} \theta_j^2 \tag{2}$$

where k_B is Boltzmann's constant, T the absolute temperature, θ_j the angle between segments $j-1$ and j, and α the bending rigidity constant. For $j = 1$, the angle is taken between segments N and 1. α is chosen in such a way that one Kuhn statistical length is divided into k segments (Frank-Kamenetskii et al., 1985). The second term in Eq. 1 is the torsional energy:

$$E_t = \frac{2\pi^2 C}{L} \cdot (\Delta Lk - Wr)^2 \tag{3}$$

where Wr is the writhe of the chain (White, 1989), L its contour length, and C the torsional rigidity. Because ΔLk is a given external parameter to the model, the expression in parentheses, $(\Delta Lk - Wr)$, can be considered as the total twist ΔTw of the DNA as measured from its equilibrium value according to the well known relation $\Delta Lk = \Delta Tw + Wr$ (White, 1989).

An ensemble of chain configurations at free-energy equilibrium is generated in this model in the following way. Starting from a configuration whose energy E_n can be calculated through Eqs. 1–3, segments of the chain are moved using a set of rules that will be described below. After each move, the energy of the new configuration E_{n+1} is calculated and compared with the previous one. If $E_{n+1} \le E_n$, the new conformation is included in the ensemble and its energy and other physical properties included in a running average. If $E_{n+1} > E_n$, the new conformation will be included only with a probability $\exp(-\Delta E/k_B T)$, where $\Delta E = E_{n+1} - E_n$; otherwise the old conformation will be counted again. This is the standard Monte Carlo algorithm (Metropolis et al., 1953).

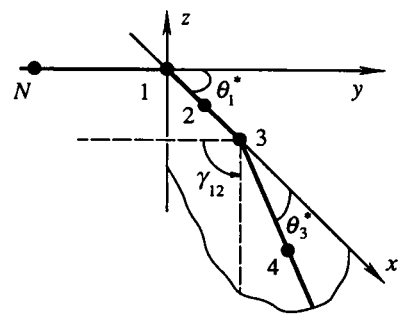

FIGURE 1 A part of the model chain at elastic equilibrium with the following parameters: $m = 2$, $l_1 = 1$, $l_2 = 3$, $\theta_1^* = \pi/2$, $\theta_3^* = \pi/4$, $\gamma_{12} = \pi/2$.

In the model described so far the chain is isotropic: the segments are straight and all bend directions at each joint are equally probable. To study the influence of permanent DNA curves on the structure of the superhelix, we have modified the basic model to represent anisotropic chains. A permanent bend can be located at any chain joint; the maximum number of bends is thus equal to the number of segments. For m bends, a set of three $m-1$ parameters is required to describe a chain shape at elastic equilibrium:

1) the numbers of the joints where the permanent bends are located:

$$1 \le l_1 < l_2 < \cdots < l_m \le N;$$

2) the bend angles:

$$0 < \theta_{l_1}^*, \theta_{l_2}^*, \cdots, \theta_{l_m}^* \le \pi;$$

3) the angles between the planes of subsequent bends:

$$-\pi < \gamma_{12}, \gamma_{23}, \cdots, \gamma_{(m-1)m} \le \pi.$$

These parameters are illustrated in Fig. 1.

The geometrical structure of the model is modified in the following way with respect to the old model. Let us denote by $\mathbf{r}_j$ ($j = 1, \cdots, N$) the positions of the chain joints; the vectors $\mathbf{e}_j = \mathbf{r}_{j+1} - \mathbf{r}_j$ are the chain segments. For each bent joint, we introduce an additional "virtual" segment $\mathbf{v}_l$ ($l = l_1, l_2, \cdots, l_m$) that is defined in such a way that the angle between $\mathbf{e}_l$ and $\mathbf{v}_l$ is fixed and equal to θ^*_l. The rotational angle ϕ_l of $\mathbf{e}_l$ around $\mathbf{v}_l$ is now a new degree of freedom. The length of $\mathbf{v}_l$ does not play an important role.

Using these conventions, the new expression for the bending energy formally coincides with Eq. 2, but the θ_j values have a different meaning in the case of bent joint. Now θ_j is the angle between $\mathbf{v}_j$ and $\mathbf{e}_{j-1}$, not between

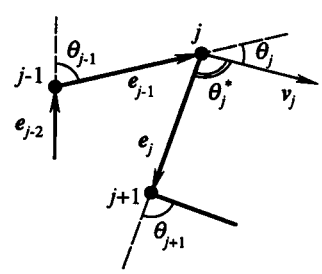

FIGURE 2 Introduction of a permanent bend between segments by definition of a virtual segment $\mathbf{v}_j$ (see text). θ_j^* is the permanent bending angle. j, bent joint; $j-1, j+1$, non-bent joints, $\theta_j^* = \pi/2$ (fixed), θ_{j-1}, θ_j, θ_{j+1}, degrees of freedom.

$\mathbf{e}_j$ and $\mathbf{e}_{j-1}$ as before ($j = l_1, l_2, \cdots, l_m$). For the remaining joints the meanings of θ_j do not change (see Fig. 2 for illustration). At elastic equilibrium, when all $\theta_j = 0$ ($j = 1, 2, \cdots, N$), the angles between the segments at the bent joints are equal to θ^*_l ($l = l_1, l_2, \cdots, l_m$). This new model geometry can be viewed as a limiting case of another possible structure, where bent segments are used instead of straight ones but the bends are shifted very closely to the joints.

For the torsion energy, Eq. 3 is no more valid because it was derived assuming that all possible distributions of the twist ΔTw over the chain length can be averaged. Now, the twist distribution is strongly restricted by the mutual orientation of the permanent bends (i.e., by the ϕ_l angles). The new expression for the torsional energy is

$$E_t = 2\pi^2 C \sum_{i=1}^{m} \frac{\Delta Tw^2_{(i-1)i}}{L_{(i-1)i}} \tag{4}$$

where $\Delta Tw_{(i-1)i}$ is the twist between subsequent permanent bends and $L_{(i-1)i}$ is the length of the corresponding chain section.

In eq. (4),

$$\Delta Tw_{01} = \Delta Lk - Wr - \sum_{i=2}^{m} \Delta Tw_{(i-1)i} \tag{4a}$$

$$L_{01} = L - \sum_{i=2}^{m} L_{(i-1)i} \tag{4b}$$

and the fractional parts of the $\Delta Tw_{(i-1)i}$ ($i = 2, \cdots, m$) values can be calculated for a given chain conformation as shown in the Appendix, whereas the integer parts are free parameters that depend on the evolution of the chain during the Monte Carlo simulation. For the starting configuration these integer parts are arbitrary and taken to be 0. For each new configuration those new values of $\Delta Tw_{(i-1)i}$ that are closest to the old ones are taken.

Criterion for end loops

For a given chain conformation, a procedure was established that allowed the automatic identification of end loops of the superhelix. We define a function $w(j)$, j being the segment number, in the following way:

$$w(j) = \frac{1}{2\pi} \int_{r_{j-q}}^{r_j} \int_{r_{j+1}}^{r_{j+q+1}} \frac{(d\mathbf{r}_1 \times d\mathbf{r}_2) \cdot \mathbf{r}_{1,2}}{|\mathbf{r}_{1,2}|^3} \tag{5}$$

where the integrals are taken over the contour of the chain.

This function is a modification of the known Gauss integral usually employed in calculating the writhe of a space curve. It gives the number of cross-overs between the two "tails" of a segment j, each consisting of q segments, averaged over all possible two-dimensional projections. We define a loop as a continuous sequence of segments for which $|w(j)| \geq w_{min}$, and the apex of the loop as the segment for which $|w(j)|$ has a maximum. In our calculation, q was set equal to 14 and $w_{min} = 1.0$. From an inspection of actual configurations, we found that the identification of a loop did not

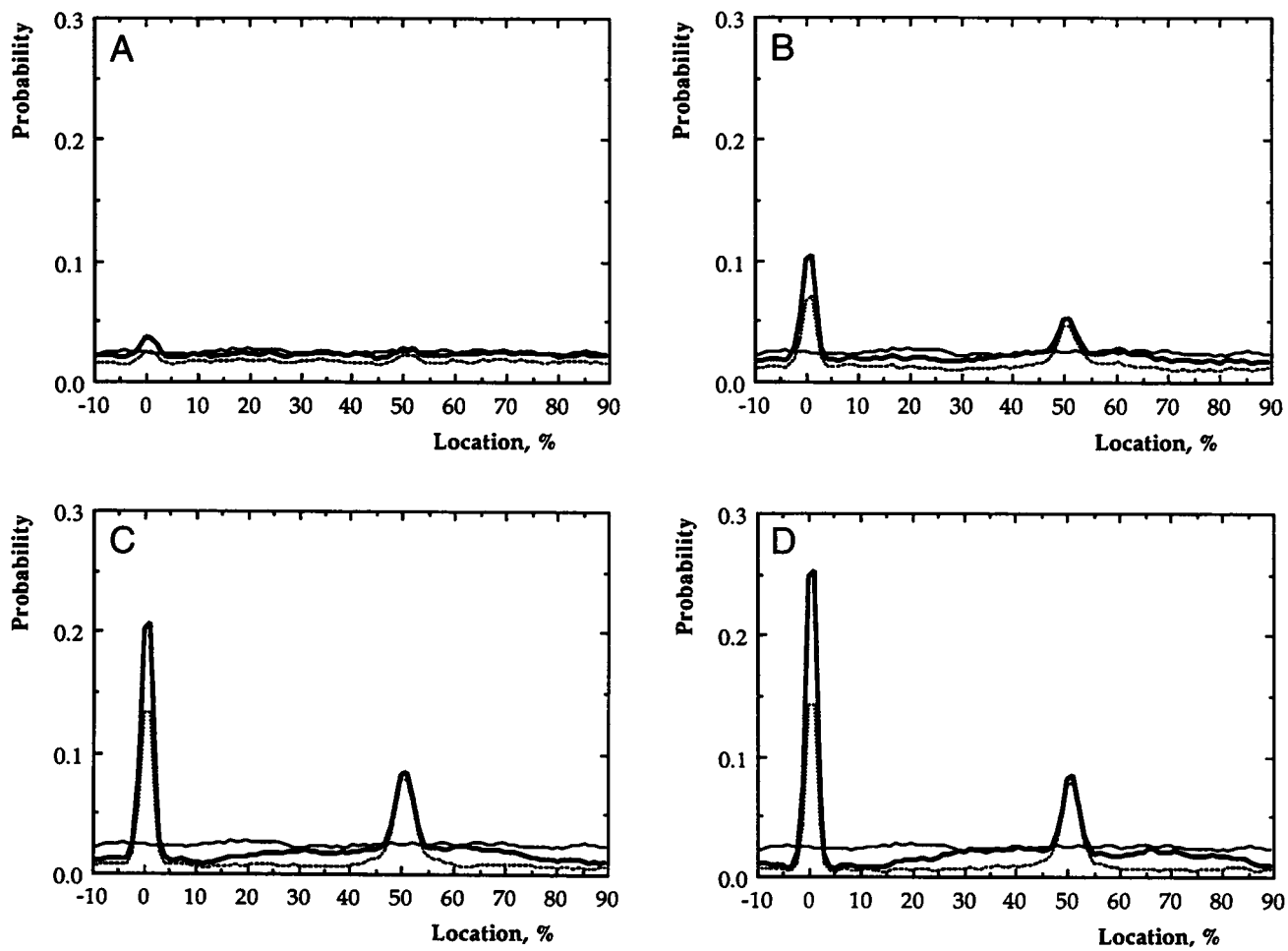

FIGURE 3 Probability distribution of the position of the loop apex in a 2694-bp superhelix with $\Delta Lk = -15$. A permanent bend was introduced at position 0. The position is given as % of the total chain length. Bending angle: 30° (*A*), 60° (*B*), 90° (*C*), 120° (*D*). Thick line: chain with permanent bend, averaged over all configurations; broken line: chain with permanent bend, averaged only over those configurations that have exactly two end loops ("straight interwound"); thin line: control without permanent bends.

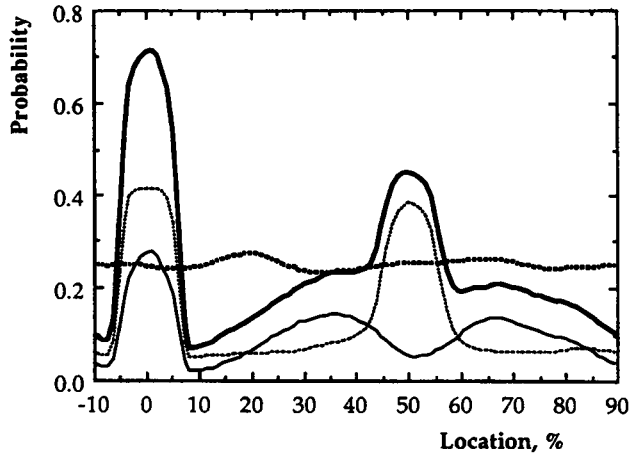

FIGURE 4 Probability distribution of a segment being included in a loop, as defined in Materials and Methods. The parameters were the same as in Fig. 3; a 120° permanent bend was introduced at position 0. Thick solid line: chain with permanent bend, averaged over all configurations; thin broken line: chain with permanent bend, averaged only over those configurations that have exactly two end loops ("straight interwound"). Thin solid line: chain with permanent bend, averaged over those configurations that have three end loops (Y-form); thick broken line: control without permanent bends.

depend very critically on q or on the threshold w_{min}, and that the error in identifying a loop was ~1%.

Parameters

For the simulations described here we used a circular DNA chain of a contour length L = 916 nm corresponding to 2694 bp, a Kuhn length b = 100 nm, and N = 96 segments. Thus, one segment corresponded to 28 bp. This set of parameters was chosen because in a parallel work we compared the simulation results with hydrodynamic data from pUC18 plasmid DNA (2687 bp), and the total chain length had to be an integer multiple of the diameter of the hydrodynamic bead, 3.18 nm (Hagerman and Zimm, 1981). The DNA effective diameter is known to vary significantly depending on ambient conditions (Shaw and Wang, 1993; Rybenkov et al., 1993). We assumed in our calculations an effective chain diameter equal to the geometrical diameter of DNA of 2 nm, which corresponds to the limit of high salt concentration (see Shaw and Wang, 1993; Rybenkov et al., 1993). The torsional rigidity was set to $C = 3.0 \cdot 10^{-19}$ erg cm, and the linking number was $\Delta Lk = -15$, corresponding to a superhelical density $\sigma = -0.058$. A permanent bend of bending angle θ was defined by setting the bending angles at three successive joints to $\theta/3$ in the same bending plane. The simulations were done with either one bend of 0–120° or two 90° bends at varying relative positions along the DNA chain.

The simulation was started from a random-walk circular chain. New configurations were then generated using the following types of moves: ⅓ of the moves were rotations of small subchains consisting of 2–10 segments

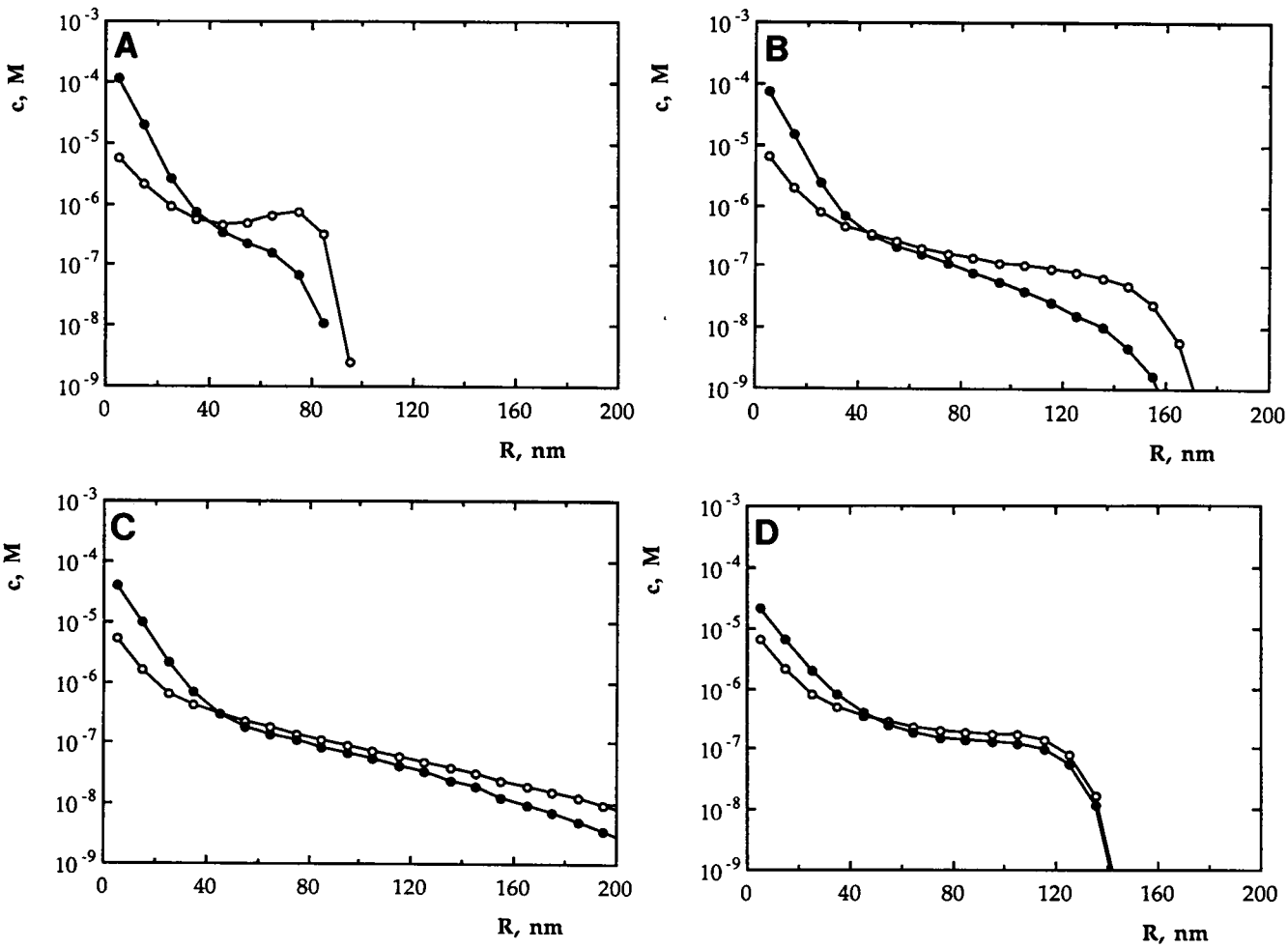

FIGURE 5 Average concentration of a DNA segment in a spherical shell with given radius and 10 nm thickness around a second segment on the other side of a permanent bend; equidistant sites, 2694-bp DNA superhelix, $\Delta Lk = -15$. Bending angle: 0° (○), 120° (●). Distance of the two sites from the center of the bend: (*A*) 140 bp, (*B*) 281 bp, (*C*) 561 bp, (*D*) 1122 bp.

around the axis connecting its end points; ⅓ of the moves were rotations of large subchains consisting of 11–48 segments. The virtual segments were rotated in the same manner as the corresponding chain segments. The last ⅓ of all moves consisted of reptational steps as described in Vologodskii et al. (1992), where subsegments of the chain are exchanged. In this case, for each of the segments exchanged, the virtual segment $\mathbf{v}_l$ was rotated around the axis $\mathbf{e}_l \times \mathbf{e}'_l$ (where $\mathbf{e}_l$ and $\mathbf{e}'_l$ are the old and new positions of the lth segment) by the angle $(\mathbf{e}_l, \mathbf{e}'_l)$. Before each of these moves, an "auxiliary move" was conducted for each virtual vector $\mathbf{v}_l$ associated with a bend, where $\mathbf{v}_l$ was rotated around $\mathbf{e}_l$ by a random angle.

For each simulation, $5 \cdot 10^6$ steps were done for equilibration, and then $3 \cdot 10^7$ steps were done for generating a sufficiently large configuration ensemble. From calculating the autocorrelation function of the loop number over successive Monte Carlo steps (Langowski et al., 1994), we verified that this ensemble size corresponded to at least 60 different branching configurations for each simulation. This and the fact that the control distribution in Figs. 3 and 4 is flat indicate that we reached convergence in our calculations. The program was written in Fortran 77 and executed on a Stardent Titan 3000.

RESULTS AND DISCUSSION

As one could anticipate, the bends significantly affect the conformations of supercoiled DNA. This is vividly demonstrated by the results of our Monte Carlo computations that follow. While discussing the results we will repeatedly refer to our previous extensive calculations performed within the framework of the original "homogeneous" model of DNA (Klenin et al., 1991; Vologodskii et al., 1992; Vologodskii and Frank-Kamenetskii, 1992).

A permanent bend is localized in the end loop of the interwound superhelix

The results of the simulations for a chain with one permanent bend are given in Fig. 3, *A–D*. Here we show the probability that a chain segment is at the apex of an end loop, as a function of its distance from the permanent bend. For increasing bending angle the end loop formation probability for the chain segments around the bend increases significantly. A particularly interesting feature of the simulation is the appearance of an "echo peak" at exactly 50% of the contour length of the chain, which comes from the second end loop of a linear interwound superhelix. Thus, the interwound structure becomes highly organized by the presence of a permanent bend.

The end loop probability can also be represented as the "integral loop probability," i.e., the probability of finding a particular chain segment somewhere in the loop (as defined in Materials and Methods). This representation is better suited to show minor features of the distribution such as variations in loop formation probability in other parts of the chain. In Fig. 4 we have analyzed the ensemble of chain conformations with a 120° permanent bend and separately displayed the contributions from superhelices with two end loops (I-form) and three end loops (Y-form). We see that the I-form almost exclusively has one end loop near the permanent bend and the other one 50% opposite it, and the loop formation probability of the DNA segments in between is very low compared with the control. The Y-form has one loop localized near the bend, and the other two loops have maximum probability at 33% and 67% of the sequence. With all configurations taken together, the loop formation probability reaches 50% of the unbent control for a distance of 20%, or 540 bp, to both sides of the permanent bend. Given that in this part of the superhelix the same DNA segments are opposite each other regardless of whether the structure is linear or branched, we can say that the permanent bend organizes ~40% of the total DNA length.

A permanent bend defines the relative orientation of distant DNA segments

To quantify the effect of the permanent bend on the long-range interactions in superhelical DNA, we have calculated the local concentration of a DNA segment in a spherical shell of given distance around another segment located at the opposite side of the permanent bend (Vologodskii et al., 1992). When the two segments are located symmetrically with respect to the permanent bend, we see a pronounced increase in the local concentration for distances ≤20 nm. The increase

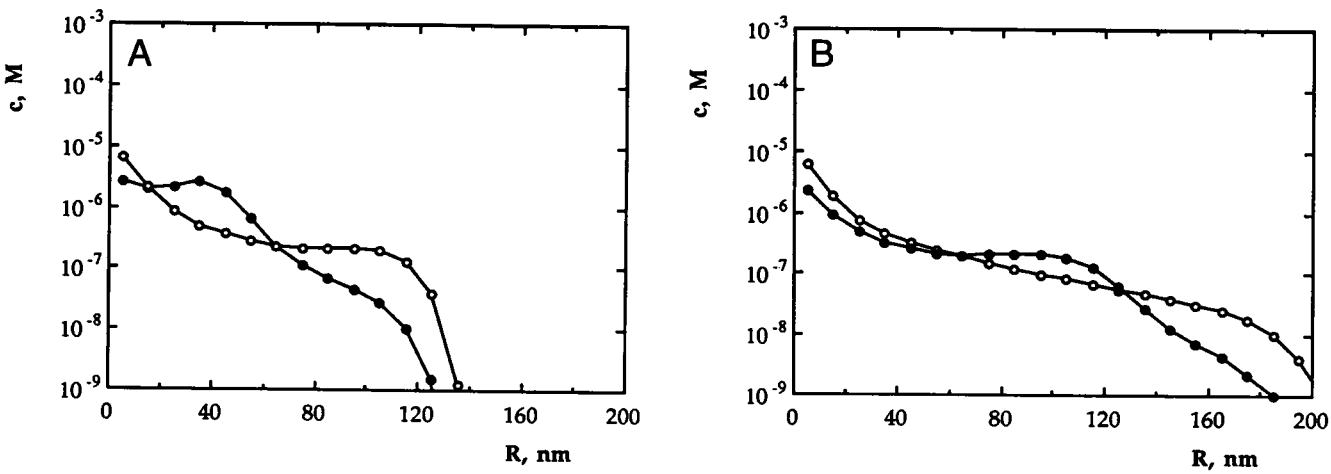

FIGURE 6 Relative local concentrations of two DNA segments as in Fig. 5; non-equidistant sites. Bending angle: 0° 0° (○), 120° (●). Distance of the two sites from the center of the bend: (*A*) 140 and 281 bp, (*B*) 140 and 561 bp.

is still visible even for DNA segments that are 1122 bp away from the center of the bend (Fig. 5, *A–D*). When the segments are asymmetrical with respect to the bend center, the interaction probability at short distances actually decreases with respect to the unbent control (Fig. 6, *A* and *B*). To show more clearly the effect of changing the bending angle, we have plotted in Fig. 7 the average concentration within an approach radius of 10 nm for two DNA segments located symmetrically or asymmetrically at different distances from a bend of varying angle. This approach radius would correspond approximately to the distance spanned by a large globular protein or a multiprotein complex that contacts different sites on the same DNA simultaneously. It is seen that for two symmetrical sites the local concentration increases dramatically with bend angle, e.g., for two sites located 140 bp from the center of a 120° bend by more than a factor of 10 compared with the unbent control. On the other hand, for asymmetrical sites 140 and 561 bp away from the bend, the interaction probability decreases by a factor of 3 when a 120° bend is introduced. Whereas for the unbent control all local concentrations are 5–6 μM, the maximum value observed for two symmetrical sites is 100 μM, and the minimum for nonsymmetrical sites 2 μM.

The relative position of bends determines the global structure of the superhelix

Because the presence of one permanent bend determines the orientation of the rest of the DNA and for an unbranched interwound superhelix the second loop can only be at 50% of the sequence with respect to the bent region, the thermodynamically favored position for a second permanent bend should be at that point. If the bend is inserted at another position, on the other hand, a branched interwound configuration might be the energetically favored one. We have conducted simulations where two 90° bends were inserted into the circle at different positions relative to each other and analyzed the configuration ensemble with respect to superhelix branching. Fig. 8 shows, as a function of distance between the two bends, the probability of unbranched (two-end), respectively Y-branched (three-end) and X-branched (four-end) configurations. While configurations with four ends occur only at a rather low percentage, which does not seem to vary with the position of the bends, the fraction of two- and three-end configuration clearly does depend on bend position. We see a maximum in the two-end configuration when the two bends are exactly 50% of the sequence apart, and a maximum in the three-end configuration when they are 33% apart. From the preceding remarks, this result is plausible. The control (Fig. 9), where we calculated the fraction of unbranched and branched configurations for one permanent bend, shows no significant dependence of the branch fraction on the bending angle.

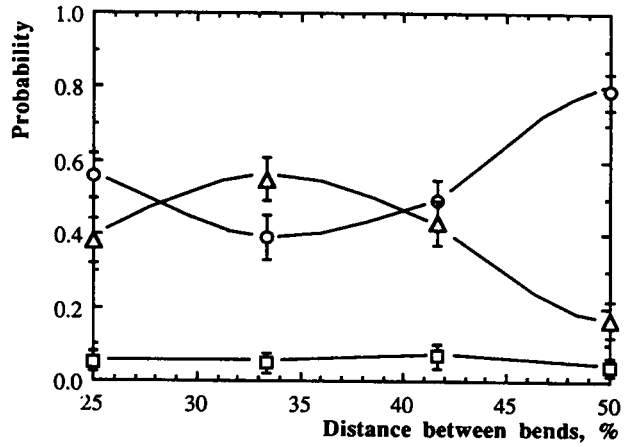

FIGURE 8 Probability of superhelix configurations with different numbers of end loops for 2694-bp DNAs ($\Delta Lk = -15$) with two permanent bends. The distance between bends is given in % of the total chain length. Number of end loops: (○) 2, (△) 3, (□) 4.

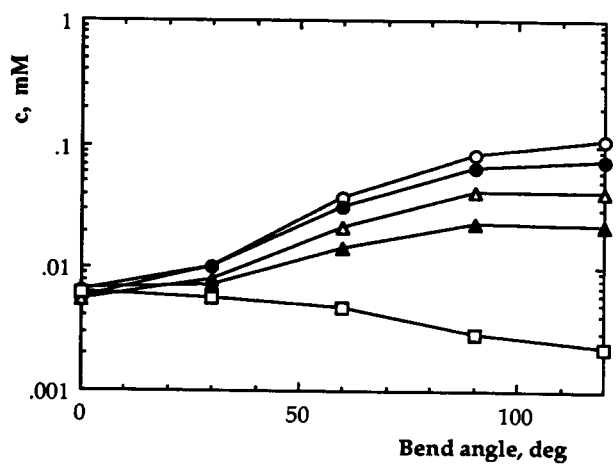

FIGURE 7 Average concentration of a DNA segment inside a 10-nm sphere around a second segment on the other side of a permanent bend. Equidistant sites: (○) 140 bp, (●) 281 bp, (△) 561 bp, (▲) 1122 bp. Nonequidistant sites: (□) 140 and 561 bp.

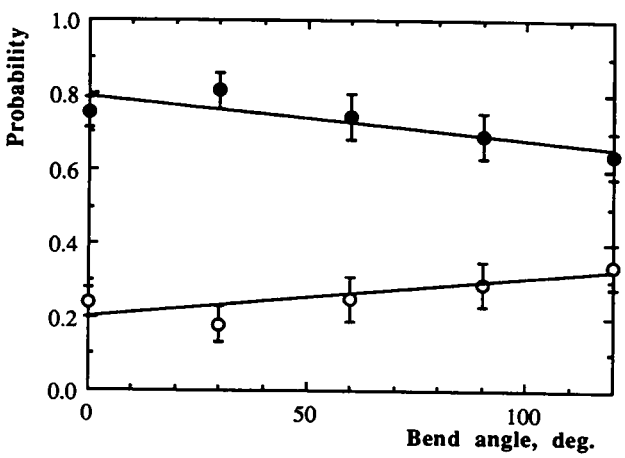

FIGURE 9 Dependence of the probability of chain branching on the presence of a permanent bend in the superhelix. (●) unbranched, (○) branched configuration with three end loops.

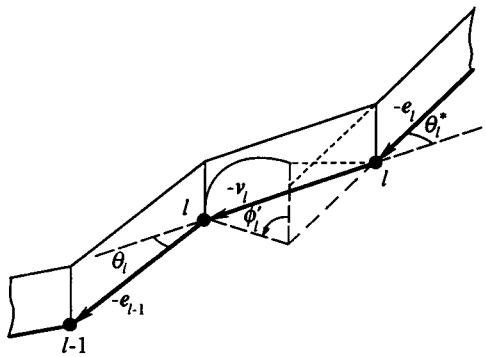

FIGURE 10 Definition of the ribbon associated with the DNA chain used to calculate the twist (see Appendix).

Energetics of the localization of the end loop

The conformational properties of a chain with the permanent bend may be also treated thermodynamically. We define a state 1 with free energy F_1 corresponding to the conformations where the bend is located somewhere within the loop, and a state 2 with free energy F_2 for the conformations where the bend is located outside the loop. The fraction of DNA belonging to the loop is equal to the width of the peaks in Fig. 4, and approximately equal to $W_1/(W_1 + W_2)$, where W_1 and W_2 are the statistical weights of states 1 and 2. The free energy gain, $\Delta F = F_2 - F_1$, due to location of the bend within the loop (state 1) as compared with state 2 may be estimated as:

$$\Delta F = F_2 - F_1 = RT \ln\left(\frac{p_1}{1 - p_1}\right),$$

where p_1 is the probability of state 1, R is the gas constant, T is the absolute temperature. From Fig. 4 we obtain $p_1 = 0.71$, so $\Delta F = 2.2$ kJ/mol. The difference in the mean energy of the two states is $\Delta E = 7.3$ kJ/mol. Although the energy used in the Monte Carlo procedure (Eqs. 1, 2, and 4) depends on the model, the ΔE value does not and has its usual physical meaning (Vologodskii et al., 1992). Therefore, the entropy of transition is $\Delta S = (\Delta E - \Delta F)/T = 17$ J mol^{-1} K^{-1}. As a result, the ratio of statistical weights of states 1 and 2 is $W_1/W_2 = \exp(-\Delta S/R) = 0.12$, which is close to the width of the main peak in Fig. 4.

CONCLUSION

Our computer simulations predict a significant effect of a local conformational change (i.e., a bend) on the global conformation of superhelical DNA. The results, obtained here for DNA circles, hold equally for topologically constrained domains of a long linear DNA. Bends can be induced in DNA in many ways, either by particular sequences (Diekmann, 1986; Koo et al., 1986) or by some DNA-binding proteins (Schultz et al., 1991). Our findings open a very interesting possibility of interplay between bends and supercoils; in particular, we would predict that the interaction probability between sequences that are located symmetrically with respect to a bend is increased over a rather long distance (up to at least 1000 bp). It is now necessary to design simple experimental systems that allow us to study intramolecular interactions in superhelical DNA. Such systems could be based, e.g., on DNA looping by multimeric proteins (Law et al., 1993; Borowiec et al., 1987), or cross-linking by bifunctional reagents. We also predict correlations between the positions of promoters, distant regulatory sites, and bent DNA sequences or binding sites for DNA-bending proteins. Whether such correlations exist remains to be established by statistical analyses of contiguous genomic sequences. We believe that our theoretical predictions will stimulate studies along these lines.

APPENDIX

Calculation of the fractional part of the twist between permanent bends

Here, for convenience, we consider the vectors $\mathbf{v}_l$ ($l = l_1, \cdots, l_m$) as very short insertions between the segments $\mathbf{e}_{l-1}$ and $\mathbf{e}_l$. Because the twist $\Delta Tw_{(i-1)i}$ ($i = 1, \cdots, m$) does not depend on the direction along the chain, it is easier to measure it from the ith bend downward to the $(i - 1)$th bend.

Let us consider a ribbon that is defined in such a way that its lower edge coincides with the chain itself and the upper edge is obtained from the chain by a very small upward shift. In Fig. 10 a part of the chain adjacent to the lth joint is shown ($l = l_1, \cdots, l_m$). Note that the inverted directions of the chain segments are used and that the distance between the two points marked by l should be infinitesimally small. The orientation of a permanent bend is given by a rotational angle ϕ_l' of the vector $-\mathbf{v}_l$ around the vector $-\mathbf{e}_l$. The angle ϕ_l' is measured from the highest possible position of $-\mathbf{v}_l$. The positive direction of rotation is measured clockwise looking in the direction of $-\mathbf{e}_l$. If $\phi_l' = 0$ then $-\mathbf{v}_l$ is in the ribbon plane corresponding to the segment $-\mathbf{e}_l$. Thus, the ribbon defines a basis for measuring the bend orientation.

The fractional part of $\Delta Tw_{(i-1)i}$ is equal to the fractional part of

$$\frac{1}{2\pi}(\phi'_{l_{i-1}} - \phi'_{l_i} - \gamma_{(i-1)i}) + \mathrm{Tw}^{\mathrm{rib}}_{(i-1)i},$$

where $Tw^{\mathrm{rib}}_{(i-1)i}$ is the twist of the ribbon between the l_{i-1}th and l_ith segments:

$$Tw^{\mathrm{rib}}_{(i-1)i} = \sum_{j=l_{i-1}+1}^{l_i} \beta_j$$

where β_j is the twist of the ribbon at the jth joint. The β_j values are determined through the Le Bret (1980) algorithm for the calculation of writhe.

This work was supported by a European Molecular Biology Organization short-term fellowship to K. K. and DFG grant La 500/4–1 to J. L.

REFERENCES

Bauer, W. R., R. A. Lund, and J. H. White. 1993. Twist and writhe of a DNA loop containing intrinsic bends. *Proc. Natl. Acad. Sci. USA.* 90:833–837.

Bednar, J., F. Furrer, A. Stasiak, J. Dubochet, E. H. Egelman, and A. D. Bates. 1994. The twist, writhe and overall shape of supercoiled DNA change during counterion-induced transition from a loosely to a tightly interwound superhelix. *J. Mol. Biol.* 235:825–847.

Borowiec, J. A., L. Zhang, S. Sasse-Dwight, and J. D. Gralla. 1987. DNA supercoiling promotes the formation of a bent repression loop in lac DNA. *J. Mol. Biol.* 196:101–111

Bracco, L., D. Kotlarz, A. Kolb, S. Diekmann, and H. Buc. 1989. Synthetic curved DNA sequences can act as transcriptional activators in *E. coli*. *EMBO J.* 8:4289–4296.

Chirico, G., U. Kapp, K. Klenin, W. Kremer, and J. Langowski. 1993. Ten microseconds in the life of a superhelix. *J. Math. Chem.* 13:33–43.

Chirico, G., and J. Langowski. 1992. Calculating hydrodynamic properties of DNA through a second-order Brownian Dynamics algorithm. *Macromolecules.* 25:769–775.

Chirico, G., and J. Langowski. 1994. Kinetics of DNA supercoiling studied by Brownian Dynamics simulation. *Biopolymers.* 34:415–433.

Crothers, D. M. 1993. Architectural elements in nucleoprotein complexes. *Curr. Biol.* 3:675–676.

Diekmann, S. 1986. Sequence specificity of curved DNA. *FEBS Lett.* 195: 53–56.

Frank-Kamenetskii, M. D., A. V. Lukashin, V. V. Anshelevich, and A. V. Vologodskii. 1985. Torsional and bending rigidity of the double helix from data on small DNA rings. *J. Biomol. Struct. Dyn.* 2:1005–1012.

Gartenberg, M. R., and D. M. Crothers. 1991. Synthetic DNA bending sequences increase the rate of in vitro transcription initiation at the *E.coli lac* promoter. *J. Mol. Biol.* 219:217–230.

Goodman, S. D., and H. A. Nash. 1989. Functional replacement of a protein-induced bend in a DNA recombination site. *Nature.* 341:251–254.

Hagerman, P., and B. H. Zimm. 1981. Monte-Carlo approach to the analysis of the rotational diffusion of wormlike chains. *Biopolymers.* 20: 1481–1502.

Hao, M.-H., and W. K. Olson. 1989. Modeling DNA supercoils and knots with B-spling functions. *Biopolymers.* 28:873–900.

Klenin, K. V., A. V. Vologodskii, V. V. Anshelevich, A. M. Dykhne, and M. D. Frank-Kamenetskii. 1988. Effect of excluded volume on topological properties of circular DNA. *J. Biomol. Struct. Dyn.* 5:1173–1185.

Klenin, K. V., A. V. Vologodskii, V. V. Anshelevich, A. M. Dykhne, and M. D. Frank-Kamenetskii. 1991. Computer simulation of DNA supercoiling. *J. Mol. Biol.* 217:413–419.

Klenin, K. V., A. V. Vologodskii, V. V. Anshelevich, V. Y. Klishko, A. M. Dykhne, and M. D. Frank-Kamenetskii. 1989. Variance of writhe for wormlike DNA rings with excluded volume. *J. Biomol. Struct. Dyn.* 4:707–714.

Koo, H. S., H. M. Wu, and D. M. Crothers. 1986. DNA bending at adenine·thymine tracts. *Nature.* 320:501–506.

Kremer, W., K. Klenin, S. Diekmann, and J. Langowski. 1993. DNA curvature influences the internal motions of supercoiled DNA. *EMBO J.* 12:4407–4412.

Langowski, J., U. Kapp, K. Klenin, and A. Vologodskii. 1994. Solution structure and dynamics of DNA topoisomers. Dynamic light scattering studies and Monte-Carlo simulations. *Biopolymers.* 34:639–646.

Laundon, H. L., and J. D. Griffith. 1988. Curved helix segments can uniquely orient the topology of supertwisted DNA. *Cell.* 52:545–549.

Law, S. M., G. R. Bellomy, P. J. Schlax, and M. T. Record. 1993. In vivo thermodynamic analysis of repression with and without looping in lac constructs. Estimates of free and local lac repressor concentrations and of physical properties of a region of supercoiled DNA in vivo. *J. Mol. Biol.* 230:161–173

Le Bret, M. 1980. Monte Carlo computation of supercoiling energy, the sedimentation constant, and the radius of gyration of unknotted and circular DNA. *Biopolymers.* 19:619–637.

Metropolis, N., A. W. Rosenbluth, M. N. Rosenbluth, A. H. Teller, and E. Teller. 1953. Equation of state calculations by fast computing machines. *J. Chem. Phys.* 21:1087–1092.

Pérez-Martín, J., and M. Espinosa. 1991. The RepA repressor can act as a transcriptional activator by inducing DNA bends. *EMBO J.* 10: 1375–1382.

Rybenkov, V. V., N. R. Cozzarelli, and A. V. Vologodskii. 1993. Probability of DNA knotting and the effective diameter of the double helix. *Proc. Natl. Acad. Sci. USA.* 90:5307–5311.

Schlick, T., and W. K. Olson. 1992. Supercoiled DNA energetics and dynamics by computer simulation. *J. Mol. Biol.* 223:1089–1119.

Schultz, S. C., G. C. Shields, and T. A. Steitz. 1991. Crystal structure of a CAP-DNA complex: the DNA is bent by 90°. *Science.* 253:1001–1007.

Shaw, S. Y., and J. C. Wang. 1993. Knotting of a DNA chain during ring closure. *Science.* 260:533–536.

Tan, R. K. Z., and S. C. Harvey. 1989. Molecular mechanics model of supercoiled DNA. *J. Mol. Biol.* 205:573–591.

Tobias, I., and W. K. Olson. 1993. The effect of intrinsic curvature on supercoiling: predictions of elastic theory. *Biopolymers.* 33:639–646.

Vologodskii, A. V., and M. D. Frank-Kamenetskii. 1992. Modeling supercoiled DNA. *Methods Enzymol.* 211:467–480.

Vologodskii, A. V., S. D. Levene, K. V. Klenin, M. D. Frank-Kamenetskii, and N. R. Cozzarelli. 1992. Conformational and thermodynamic properties of supercoiled DNA. *J. Mol. Biol.* 227:1224–1243.

White, J. H. 1989. An introduction to the geometry and topology of DNA structure. *In* Mathematical Methods for DNA Sequences. M. S. Waterman, editor. CRC Press, Boca Raton, FL. 222–253.

Yang, Y., I. Tobias, and W. K. Olson. 1993. Finite element analysis of DNA supercoiling. *J. Chem. Phys.* 98:1673–1686.